Available online at www.sciencedirect.com
ScienceDirect
Catalysis Communications 9 (2008) 101–105
CATALYSIS COMMUNICATIONS
www.elsevier.com/locate/catcom

NO reduction by H_2 over nano-$Ce_{0.98}Pd_{0.02}O_{2-\delta}$

Sounak Roy [a], A. Marimuthu [b], M.S. Hegde [a], Giridhar Madras [b,*]

[a] Solid State and Structural Chemistry Unit, Indian Institute of Science, Bangalore 560 012, India
[b] Chemical Engineering Department, Indian Institute of Science, Bangalore 560 012, India

Received 11 April 2007; received in revised form 10 May 2007; accepted 14 May 2007
Available online 31 May 2007

Abstract

Development of new catalysts for controlling nitrogen oxides (NO_x) emissions is an important technical challenge as increasingly strict emission limits are being imposed. A new catalyst Pd^{2+} substituted CeO_2 ($Ce_{0.98}Pd_{0.02}O_{2-\delta}$) was synthesized by solution combustion method. The material was characterized by XRD, TEM and XPS and used to investigate the reduction of NO by H_2. The catalyst shows 100% N_2 selectivity at low temperature and thus is superior to other catalysts reported in literature. A bifunctional reaction mechanism has been proposed to model the experimental data.

Keywords: De-NO_x reaction by H_2; Pd^{2+}doped CeO_2; Reaction mechanism

1. Introduction

Most of the combustion processes result in NO_x formation. Nitrogen oxides (NO_x) are serious environmental pollutants and the emissions of these compounds need to be strictly regulated. Reduction of NO_x can be accomplished by using ammonia or hydrocarbons as reductants. However, these methods result in other environmental issues and thus the use of hydrogen as a reductant for the NO reduction may be favorable. Therefore, several studies [1–7] have investigated the use of various noble metal catalysts for the reduction of NO by H_2. Though the overall conversion of NO over H_2 is higher over Pt based catalysts than Rh based catalysts, the selectivity of N_2 is lower over Pt. However, there are restrictions on the use of Rh and there is an immediate need to develop Rh-free automotive catalyst [1]. Thus, recent studies have investigated the effects of the addition of metal oxides as a promoter or co-catalyst to Pt or Pd. This includes studies with Pt/SiO_2 [1], Pt/Al_2O_3 [3], etc., but the selectivity of N_2 was low. The use of Pd for $NO + H_2$ has not been extensively studied and only few studies [5,6] have used Pd dispersed on Al_2O_3. However, we have shown that Pd substituted on reducible supports like CeO_2, TiO_2, etc., show higher catalytic activity compared to that Pd dispersed on Al_2O_3 for the NO + CO reaction [8,9]. Based on this observation, this study investigates the application of Pd/CeO_2 catalyst on the reduction of NO by H_2. A bifunctional mechanism has been proposed to model the experimental data and determine the kinetics.

2. Experimental

2.1. Preparation of catalysts

$Ce_{0.98}Pd_{0.02}O_{2-\delta}$ has been prepared by a single step solution combustion method [8,9]. The combustion mixture contained $(NH_4)_2Ce(NO_3)_6$, $PdCl_2$, and the fuel $C_2H_6N_4O_2$ (oxalyldihydrazide, ODH) in the molar ratio 0.98:0.02:2.352. In a typical synthesis, 10 g of $(NH_4)Ce(NO_3)_6$, 0.066 g of $PdCl_2$ (Ranbaxy Laboratories Ltd., 99%), and 5.175 g of ODH were dissolved in the minimum volume of water in a borosilicate dish and introduced into a muffle furnace maintained at 350 °C. The solution initially boiled with frothing and foaming and underwent dehydration. At the point of complete dehydration, the

* Corresponding author. Tel.: +91 80 2293 2321; fax: +91 80 2360 0683.
E-mail address: giridhar@chemeng.iisc.ernet.in (G. Madras).

1566-7367/$ - see front matter © 2007 Elsevier B.V. All rights reserved.
doi:10.1016/j.catcom.2007.05.031

surface ignited, burning with a flame (~1000 °C) and yielding a voluminous solid product within 5 min. Though $PdCl_2$ was used in the synthesis, no chlorine was present in the catalyst.

2.2. Characterization of catalysts

Powder X-ray diffraction (XRD) patterns of oxide samples were recorded on a Phillips X'Pert diffractometer using Cu Kα radiation at a scan rate of $2\theta = 0.5°$/min before and after the catalytic reactions. X-ray photoelectron spectra (XPS) of the as prepared catalysts and used catalysts were recorded on an ESCA-3 Mark II VG scientific spectrometer using Al Kα radiation (1486.6 eV). Binding energies reported are with respect to C (1s) at 285 eV and were measured with a precision of ±0.2 eV.

Hydrogen uptake experiments as a function of temperature were carried out by passing H_2 over 50 mg of catalyst. A TCD detector detects the amount of H_2 uptake.

2.3. Catalytic tests

The catalytic reactions were investigated in a temperature programmed reaction system equipped with a quadrupole mass spectrometer SX200 (VG Scientific Ltd., England). The catalyst samples were packed in a reactor, inserted into a furnace heated to required reaction temperature measured by chromel–alumel thermocouple dipped in the catalyst bed through a temperature controller. The gaseous products were sampled by a quadrupole mass spectrometer. Typically 60–40 mesh of catalyst is used with SiO_2 to make up the catalyst bed volume 0.138 cc. Flow rate was 100 sccm with GHSV = 43,000 h^{-1}. Gases are from M/S Bhuruka Gases Ltd. (India) with 4.74 vol% NO in He, 10.49 vol% H_2 in He and 99.99% pure O_2 in this study.

3. Results

3.1. Structural studies

Detailed structure of 1–2 atom% Pd ion doped CeO_2 has been reported earlier [8,9]. The combustion synthesized Pd/CeO_2 consists of Pd^{2+} ion substituted $Ce_{0.98}Pd_{0.02}O_{2-\delta}$ solid solution. CeO_2 crystallizes in fluorite structure. Reflections due to PdO and Pd° metal particles have not been observed (Fig. 1a). Crystallite sizes were in the range of 30–40 nm, as determined from Scherrer formula, and confirmed by TEM. Representative TEM images with the corresponding ED pattern of Pd/CeO_2 catalysts are shown in Fig. 1b. No Pd metal is seen in the TEM image of the 2-atom% Pd/CeO_2. The cubic crystallites are in the range of 30–40 nm and no diffraction ring or spot other than that of ceria is found in the ED pattern of the same. This TEM study demonstrates that Pd is dispersed as ionic in CeO_2. The importance of the nature of the support has demonstrated earlier [8,10]. Because of the ionic character of substituted Pd, there must be oxide ion vacancies in the CeO_2 support. The vacancies on the surface of the support influence the adsorption and dissociation of NO, as discussed in the reaction mechanism below. XPS of Pd (3d) region of $Ce_{0.98}Pd_{0.02}O_{2-\delta}$ confirms the ionic character of substituted Pd^{2+} in CeO_2 (Fig. 1c).

3.2. H_2 uptake studies

H_2-TPR profile of $Ce_{0.98}Pd_{0.02}O_{2-\delta}$ is given in Fig. 1d. The peak at 101 °C is attributed to the reduction of Pd^{2+} ions in CeO_2. Total amount of H_2 taken up by Pd^{2+} in CeO_2 has been estimated from the integrated area under the peak and the hydrogen to palladium mole ratio is close to 3. This means that part of Ce^{4+} gets reduced at this low temperature. This is because, if only Pd^{2+} ion was reduced, H_2/Pd ratio should be equal to unity for $Pd^{2+} + H_2 \rightarrow Pd^0 + 2H^+$ reaction.

3.3. NO–H_2 reaction

NO reduction with hydrogen was carried out with NO:H_2 ratio of 1:1 vol% and 1:3 vol% for the catalysts $Ce_{0.98}Pd_{0.02}O_{2-\delta}$. The light off curve has been shown in Fig. 2a and b. When the feed gas is stoichiometric (NO:H_2 = 1:1 vol%), complete conversion of NO takes place only at around 300 °C but when NO:H_2 = 1:3 vol%, complete conversion of NO occurs at 180 °C itself.

3.4. Model for NO–H_2 reaction

Many monofunctional mechanisms have been proposed [1,14] in the literature for NO reduction by H_2 over noble metals supported on non-reducible oxides like SiO_2/Al_2O_3. In our earlier studies, we have confirmed the role of reducible ceria supports in the kinetics of $CO + O_2$, $N_2O + CO$ and $NO + CO$ reactions by using a bifunctional mechanism [8,11,12]. The following bifunctional mechanism, where the adsorption and the reaction take place both in the metal site and on the ionic vacancy of the support, is proposed. "O" and "V" are the oxide ion and vacant site, respectively, on the support and S_{Pd} is the active site on the palladium metal surface.

$$H_2 + 2S_{Pd} \Longleftrightarrow 2H_{Pd} \quad (1)$$

$$NO + S_{Pd} \Longleftrightarrow NO_{Pd} \quad (2)$$

$$NO + \text{“V”} \Longleftrightarrow N\text{“O”} \quad (3)$$

$$NO_{Pd} + N\text{“O”} \rightarrow N_2O + \text{“O”} + S_{Pd} \quad (4)$$

$$H_{Pd} + \text{“O”} \rightarrow \text{“O”}H + S_{Pd} \quad (5)$$

$$\text{“O”}H + H_{Pd} \rightarrow H_2O + \text{“V”} + S_{Pd} \quad (6)$$

$$N_2O + \text{“V”} \rightarrow N_2 + \text{“O”} \quad (7)$$

Step 1 represents the adsorption of H_2 on the Pd site. Steps (2) and (3) refer to the adsorption of NO on Pd and the vacancy site, respectively. The adsorption of NO on the vacancy has also been demonstrated to occur on unsubstituted CeO_2 [13]. The formation of N_2O (step 4)

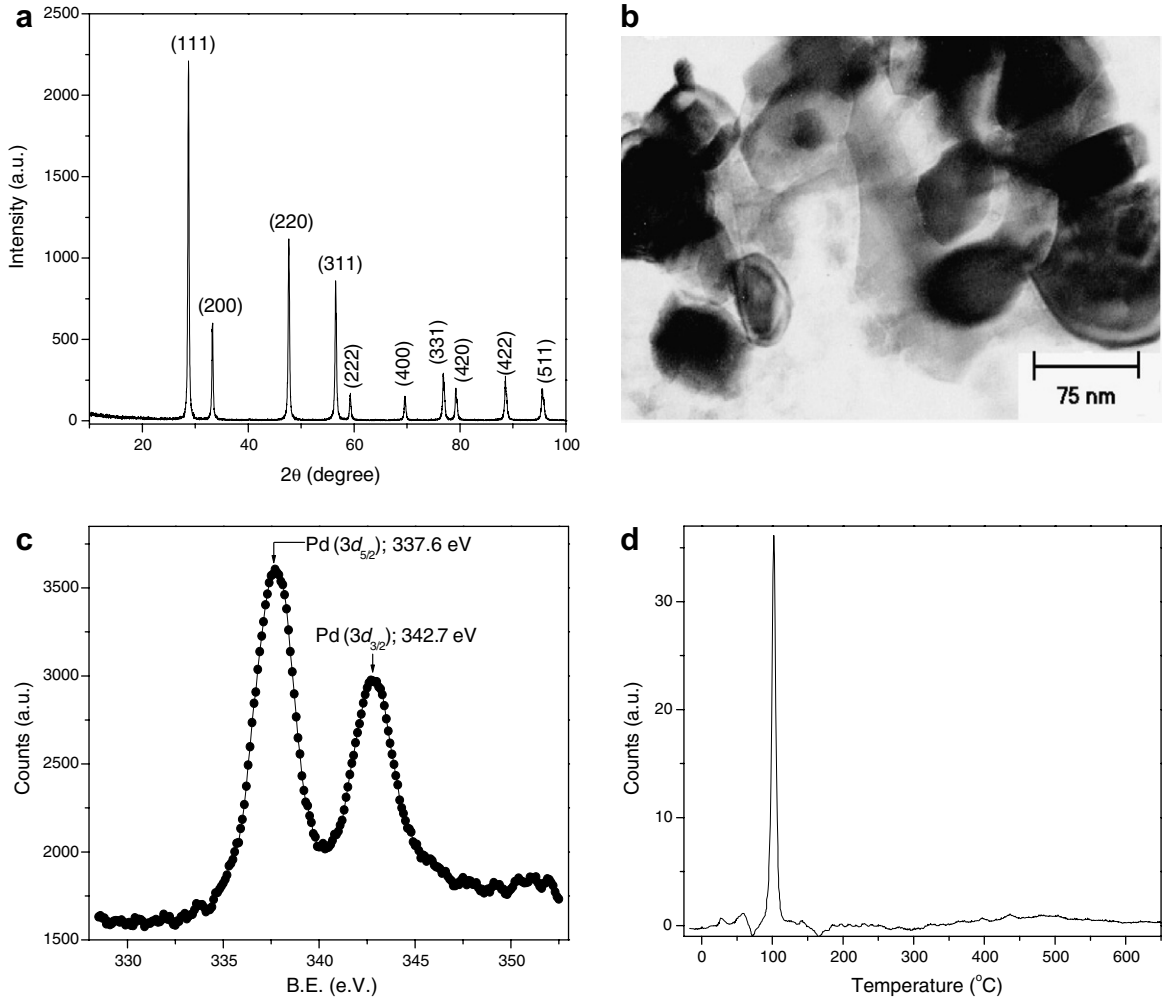

Fig. 1. (a) XRD pattern, (b) Pd (4d) core-level XPS, (c) TEM and (d) H_2-TPR profile of $Ce_{0.98}Pd_{0.02}O_{2-\delta}$.

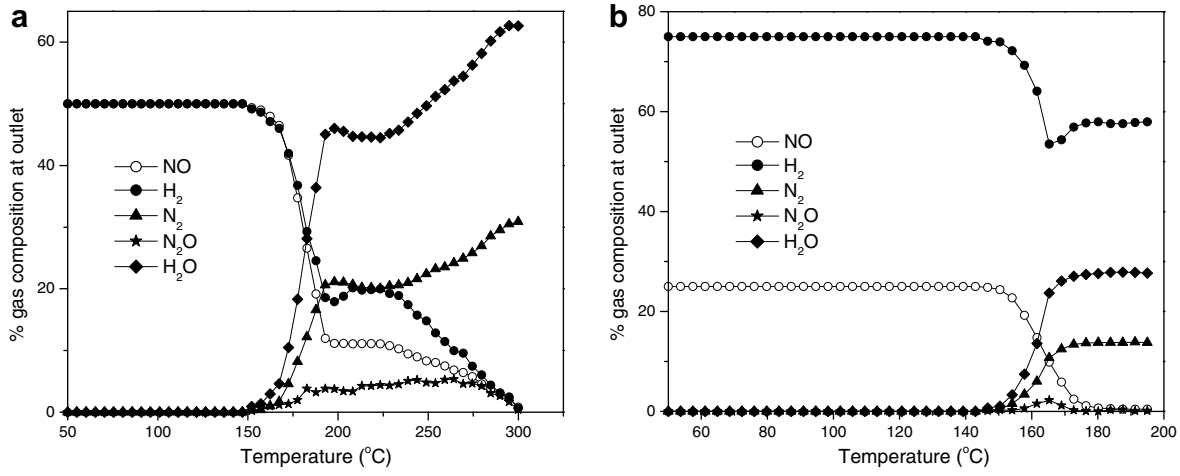

Fig. 2. TPR profile of NO + H_2 reaction over $Ce_{0.98}Pd_{0.02}O_{2-\delta}$. (a) NO:$H_2$ = 1:1 vol% and (b) NO:H_2 = 1:3 vol%.

occurs because of close proximity of nitrogen atom of NO_{Pd} and the nitrogen atom of N"O" adsorbed on vacancy site through "O". The hydrogen atom from the metal surface reacts with oxide ion from the easily reducible support to form water in two steps (steps 5 and 6). Some studies [1–4] show that NO dissociation takes place through N_{Pd} and O_{Pd} species followed by nitrogen gas formation from the combination of two nitrogen atoms and

the formation of NH_3 from the species N_{Pd} and H_{Pd} through different kind of intermediates. However, the evolution of NH_3 was not observed in our experiments. This is similar to that observed by Thomas et al. [14] where the reaction products were N_2 and N_2O without the evolution of NH_3. This indicates that N_2 formation (step 7) with the absence of N_{ads} is through the direct dissociation of N_2O to fill the ionic vacancy created by the strong reducing agent H_{Pd}. Our earlier studies [8,11,12] also indicate a similar mechanism for N_2 formation for NO + CO and N_2O + CO reactions.

The kinetic parameters can be predicted using a model, which can be derived from the above bifunctional mechanism. From the overall reaction stoichiometry the rate of disappearance of NO is $r_{NO} = 2(r_{N_2} + r_{N_2O})$. The rate of formation of N_2 and N_2O can be written as $r_{N_2} = k_7 C_{N_2O} \Theta_{V_2}$ and $r_{N_2O} = k_4 \Theta_{NO_1} \Theta_{NO_2}$, respectively, Θ_{V_2} refers to fractional vacant site on the support. By assuming Langmuir adsorption isotherm for both H_2 and NO on the metal surface, the fraction of sites occupied by the H and NO species on the metal surface, $\Theta_H = \frac{\sqrt{K_1 C_{H_2}}}{1+\sqrt{K_1 C_{H_2}}+K_2 C_{NO}}$ and $\Theta_{NO_1} = \frac{K_2 C_{NO}}{1+\sqrt{K_1 C_{H_2}}+K_2 C_{NO}}$. By assuming equilibrium adsorption of NO on the support for step 3, $\Theta_{NO_2} = K_3 C_{NO} \Theta_{V_2}$ The total species balance on the support is $\Theta_{v_2} + \Theta_O + \Theta_{NO_2} + \Theta_{OH} = 1$. The final expression for r_{NO},

$$r_{NO} = \frac{2[k_7 C_{N_2O} + K_2 K_3 k_4 C_{NO}^2/(1+\sqrt{K_1 C_{H_2}} + K_2 C_{NO})]}{1 + K_3 C_{NO} + \frac{(k_6+k_5)}{k_6 k_5 \sqrt{K_1 C_{H_2}}}\left[K_2 K_3 k_4 C_{NO}^2 + \frac{k_7 C_{N_2O}}{1+\sqrt{K_1 C_{H_2}}+K_2 C_{NO}}\right]} \quad (A)$$

The reaction rate for NO observed experimentally is fitted to the model with the values for K_1 and K_2 taken from Park et al. [15] and Cho [16], respectively. Fig. 3 shows the experimental and model fitting for NO + H_2 reaction. The values of the optimized rate parameters are given in Table 1.

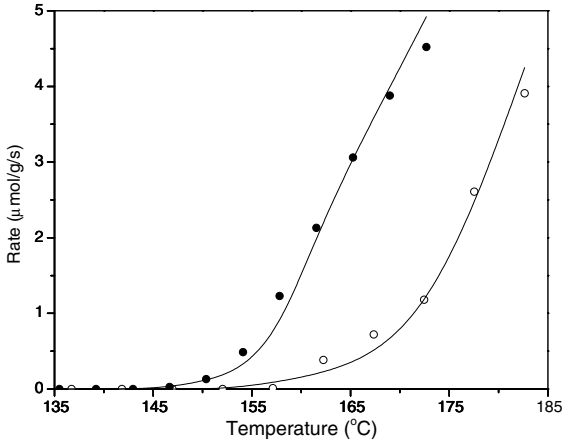

Fig. 3. Variation of NO + H_2 reaction rate with temperature with the model fit over $Ce_{0.98}Pd_{0.02}O_{2-\delta}$. The closed circles represent the reactant ratio of NO:H_2 of 1:3 vol%, while the open circles represent the experimental data for the reactant ratio of NO:H_2 of 1:1 vol%. The lines represent the model fit to the experimental data.

Table 1
Reaction rate coefficients for NO–H_2 reaction

Optimized parameter	
K_1 ($cm^3\ mol^{-1}$)	$2.058 \times 10^6 \sqrt{T}\ \exp(10000/T)$
$K_2 = K_3$ ($cm^3\ mol^{-1}$)	$10600\sqrt{T}\exp(13{,}000/T)$
k_4 (mol $g^{-1}\ s^{-1}$)	$1.207 \times 10^8 \exp(-17{,}900/T)$
k_5 (mol $g^{-1}\ s^{-1}$)	$3.849 \times \exp(-4400/T)$
k_6 (mol $g^{-1}\ s^{-1}$)	$4.962 \times 10^{10} \exp(-2000/T)$
k_7 ($cm^3\ g^{-1}\ s^{-1}$)	$8.51 \times 10^{14} \exp(-1600/T)$

The above Eq. (A) indicates that as the hydrogen concentration increases the rate of dissociation of NO increases. This is consistent with our experimental data (Fig. 3) and the experimental data reported by other investigators [2].

4. Discussion

From the experimental findings it is clear that the rate of reaction for NO:H_2 = 1:3 in the feed is more when compared to NO:H_2 = 1:1. Even though the increase in hydrogen concentration leads to the decrease in NO coverage (in step 2) on the metal site, because of the competitive adsorption, the adsorbed hydrogen atom will react with the oxide ion (in steps 5 and 6) to produce more vacant sites on the support which will increase the rate of dissociation of NO through steps 3 and 7.

By comparing the rate constants for the individual steps from Table 1, it can be concluded that N_2O formation (step 4) is the slowest step in the mechanism and N_2 formation (i.e. N_2O dissociation) is faster than step 4. This indicates that as soon as N_2O is formed, it will dissociate into N_2 and leads to more N_2 selectivity and less N_2O selectivity. The reduction reaction steps 5 and 6 are also faster than step 4, so that these two steps will consume the oxide ions and leave the ionic vacant sites on the support. However, N_2O dissociation is faster than steps 5 and 6 such that oxide vacancies are replenished and the synergism process remains intact.

The N_2 selectivity over N_2O is always higher over $Ce_{0.98}Pd_{0.02}O_{2-\delta}$, and the N_2 selectivity is higher than that of reported catalysts in available literature. Mergler and Nieuwenhuys [1] over Pt/SiO_2 and also over $Pt/CoO_x/SiO_2$ has shown N_2O selectivity is more than N_2 selectivity at low temperature, while with the increase in temperature N_2 selectivity proceeds over N_2O selectivity. Hecker and Bell [17] have also observed the same trend over Rh/SiO_2. Over Pt and Rh/Pt single crystals [18] the selectivity of N_2/N_2O is only 50%. Barrera et al. [19] has shown that N_2 selectivity in NO + H_2 reaction never exceeds 60% over $Pd/Al_2O_3/La_2O_3$, and drops to below 30% at higher temperature.

5. Conclusion

The catalyst, $Ce_{0.98}Pd_{0.02}O_{2-\delta}$, was synthesized by solution combustion method and characterized. It was used for the reduction of NO by H_2. The effect of excess H_2

was investigated. When $NO:H_2 = 1:1$, N_2O remains in the reaction medium up to 300 °C and when $NO:H_2 = 1:3$, N_2O converts to N_2 completely at 180 °C. Because of high reducibility of this material, we have shown that this catalyst shows 100% N_2 selectivity and very high reaction rates at a lower temperature compared to existing catalysts. Based on the structural studies and reaction mechanisms, we have been able to prove that the oxide vacancy in the support plays a pivotal role in determining the reaction rates. A new bifunctional mechanism based on NO and H_2 adsorption on Pd^{2+} and NO dissociation on vacancy site were proposed to model the experimental data.

Acknowledgements

The authors thank the department of science and technology, India, for financial support.

References

[1] Y.J. Mergler, B.E. Nieuwenhuys, Appl. Catal. B: Environ. 12 (1997) 95.
[2] C.A. de Wolf, B.E. Nieuwenhuys, Catal. Today 70 (2001) 287.
[3] R. Burch, M.D. Coleman, Appl. Catal. B: Environ. 23 (1999) 115.
[4] R. Burch, Catal. Today 35 (1997) 27.
[5] F. Dhainaut, S. Pietrzyk, P. Granger, Appl. Catal. B: Environ. 70 (2007) 100.
[6] T.E. Hoost, K. Otto, K.A. Laframboise, J. Catal. 155 (1995) 303.
[7] B. Frank, G. Emig, A. Renken, Appl. Catal. B: Environ. 19 (1998) 45.
[8] S. Roy, A. Marimuthu, M.S. Hegde, G. Madras, Appl. Catal. B: Environ. 71 (2006) 23.
[9] P. Bera, K.R. Priolkar, A. Gayen, P.R. Sarode, M.S. Hegde, S. Emura, R. Kumashiro, V. Jayaram, G.N. Subbana, Chem. Mater. 15 (2003) 2049.
[10] M. Gabrovska, J. Krstic, R. Edreva-Kardjieva, M. Stankovic, D. Jovanovic, Appl. Catal. A: Gen. 299 (2006) 73.
[11] S. Roy, A. Marimuthu, M.S. Hegde, G. Madras, Appl. Catal. B: Environ. 73 (2007) 300.
[12] T. Baidya, A. Marimuthu, M.S. Hegde, N. Ravishankar, G. Madras, J. Phys. Chem. B 111 (2007) 830.
[13] A. Martinez-Arias, J. Soria, J.C. Conesa, X.L. Seoane, A. Arcoya, R. Catalufia, J. Chem. Soc. Faraday. Trans 91 (1995) 1679.
[14] C. Thomas, O. Gorce, C. Fontaine, J.M. Krafft, F.O. Villain, G.D. Mariadassou, Appl. Catal. B: Environ. 63 (2006) 201.
[15] Y.K. Park, P. Aghalayam, G.D. Vlachos, J. Phys. Chem. A 103 (1999) 8101.
[16] B.K. Cho, J. Catal. 148 (1994) 697.
[17] W.C. Hecker, A.T. Bell, J. Catal. 92 (1985) 247.
[18] K. Tanaka, A. Sasahara, J. Mol. Catal. A: Chem. 155 (2000) 13.
[19] A. Barrera, M. Viniegra, P. Bosch, V.H. Lara, S. Fuentes, Appl. Catal. B: Environ. 34 (2001) 97.